Sensors & Diagnostics

PAPER

View Article Online
View Journal | View Issue

Cite this: *Sens. Diagn.*, 2023, **2**, 1286

Polymersome-based ion-selective nano-optodes containing ionophores†

Yunxin Cui,[a] Jingying Zhai,[b] Yifu Wang[a] and Xiaojiang Xie *[a]

Received 2nd June 2023,
Accepted 7th July 2023

DOI: 10.1039/d3sd00133d

rsc.li/sensors

Nanoscale ion-selective optodes (nano-ISOs) are versatile optical ion sensing tools with ionophores, ion exchangers, optical signal transducers, and sometimes plasticizers. Nano-ISOs were previously developed based on various nanoparticles with a topological solid core to contain the active sensing components. In this work, polymersomes, with a topologically hollow structure, were utilized as the matrix of nano-ISOs. Ca^{2+}-selective polymersomes with high selectivity and a sub-micromolar detection limit were developed with a calcium ionophore and successfully used to determine the total calcium concentration in diluted human serum. With a sodium ionophore, Na^{+}-selective polymersomes were also obtained, indicating that ionophore-based polymersomes are promising in forming a general ion-selective optical sensing platform.

Introduction

Ion-selective optodes (ISOs), the counterpart of ion-selective electrodes (ISEs), have enabled highly selective ion sensing relying on optical signals rather than electrochemical signals. Typically, lipophilic polymeric films and micro/nanoparticles are used to incorporate the sensing components, including ionophores, ion exchangers, and H^{+} chromoionophores (or other signal transducers).[1–7] Particularly, nanoscale ion-selective optodes (nano-ISOs) have emerged recently and attracted much attention due to their low sample consumption, fast response, and potential applications in cellular imaging.[8–11] Over the years, ionophore-based optical sensing principles[12–14] and detection modes[15,16] were extensively investigated. In addition to broadening the types of ion carriers and signal transducers, new substrate materials are also being explored to adapt to different application scenarios and improve the sensing performance of sensors.[7]

Classical nano-ISOs were previously fabricated with a combination of polymeric surfactants (Pluronic® F-127, PS-PEO, *etc.*) and plasticizers (DOS, NPOE, *etc.*). The former enabled the sensor to disperse uniformly and stably in the aqueous phase, while the latter acted as a solvent to better load the lipophilic sensing components.[7,8] In 2013, the Bakker group prepared Na^{+}-selective optodes[17] based on nanospheres *via* self-assembly of Pluronic® F-127 and DOS and then further extended them to other target analytes.[18] Recently, they also reported magnetic K^{+}-selective optodes using commercial polystyrene (PS) microspheres which were able to eliminate the scattering interference observed in traditional absorbance measurements. The analysis of the magnetic K^{+}-selective optode response was realized with an imaging camera by accumulating the sensing beads onto the detection zone in a flow system.[19] In another work, Clark *et al.* introduced organic quantum dots (ITK organic 655) into the core of a polymeric matrix and coated the nanospheres with polyethylene glycol (PEG) to improve the signal intensity, sensitivity, and biocompatibility of Na^{+}-selective optodes. A ratiometric response was obtained by adding a second quantum dot.[20] Lately, our research group presented the fabrication of bio-compatible Na^{+}- and K^{+}-selective optodes based on organosilicon nanoparticles without plasticizers,[21] PS-*g*-PEO block copolymers,[22] or graphene quantum dots.[23]

While it has been recognized that improving the biocompatibility of nano-optodes is essential for further *in vivo* applications, some nanomaterials commonly used in *in vivo* imaging and drug delivery, such as liposomes and polymer vesicles (also called polymersomes),[24] have not received much attention in the ion-selective sensor field. There were indeed some reports on the use of lipids as matrix materials to construct ion-selective optodes (Cash group,[25] Michalska group[26]), but surprisingly few studies were found to use polymersomes as the matrix of nano-ISOs though polymersomes have better mechanical stability and chemical modifiability than liposomes.[27] Besides, the unique lumen structure inside the hydrophobic membrane provides vesicles with more possibilities such as multiple sensing of

[a] *Department of Chemistry, Southern University of Science and Technology, Shenzhen, 518055, China. E-mail: xiexj@sustech.edu.cn*
[b] *Academy for Advanced Interdisciplinary Studies, Southern University of Science and Technology, Shenzhen, 518055, China*

† Electronic supplementary information (ESI) available: Size exclusion chromatography, spectra of interfering ions, data for real sample analysis with nano-optodes and ISEs. See DOI: https://doi.org/10.1039/d3sd00133d

different analytes and combination of sensing and drug delivery. Also, there is much less variation in the effective size of the sensors because the thickness of the polymersome membrane is more uniform compared with the diameter of previous ion-selective nanospheres.

In the past few years, polymersomes formed by self-assembly of the PMOXA–PDMS–PMOXA (ABA) triblock copolymer were extensively investigated.[28,29] They were demonstrated to have low permeability to water[30] and various ions,[31,32] but still exhibit highly selective transmembrane transportation by encapsulating biological proteins such as FhuA,[33] Aqpz,[30] OmpF,[34] *etc.* Palivan's group achieved transmembrane transport of Na^+ and K^+ by inserting gramicidin (gA) biopores into membranes,[35] and the effect of polymeric membrane thickness on the transmembrane transport of Ca^{2+} by inserting ionomycin was systematically investigated.[36]

In this work, we propose polymersomes as the matrix to load lipophilic chemical sensing components and investigated the optical response of the polymersome-based nano-ISOs. Concentrations of Ca^{2+} and Na^+ were detected respectively with great selectivity. As a preliminary application, the total calcium level in human serum was determined successfully, demonstrating the practical potential of polymersome-based nano-ISOs in clinical ion sensing.

Experimental section

Materials

Poly(2-methyl-2-oxazoline)-*b*-poly(dimethylsiloxane)-*b*-poly(2-methyl-2-oxazoline) (M_n = 700-*b*-5000-*b*-700, M_w/M_n = 1.3, ABA) was purchased from Polymersource. Dodecyl 2-nitrophenyl ether (DD-NPE), polyvinylchloride (PVC), tetrahydrofuran (THF), *N*,*N*-dicyclohexyl-*N*′,*N*′-dioctadecyl-3-oxapentanediamide (calcium ionophore IV, Ca IV), 4-*tert*-butylcalix[4]arene-tetraacetic acid tetraethyl ester (sodium ionophore X, Na X), 3-octadecanoylimino-7-(diethylamino)-1,2-benzophenoxazine (chromoionophore I, CH I), sodium tetrakis-[3,5-bis(trifluoromethyl)phenyl]-borate (NaTFPB), 2-amino-2-hydroxymethylpropane-1,3-diol (Tris base), sulforhodamine B (SRB), ethanol (EtOH), calcium chloride ($CaCl_2$), sodium chloride (NaCl), potassium chloride (KCl) and lithium chloride (LiCl) were purchased from Sigma-Aldrich. Magnesium chloride hexahydrate ($MgCl_2{\cdot}6H_2O$), ethylene glycol-bis(β-aminoethyl ether)-*N*,*N*,*N*′,*N*′-tetraacetic acid (EGTA), and Sephadex G-25 superfine beads were purchased from J&K Scientific Ltd. (China). The serum samples were provided by the Qian Xi Nan People's Hospital and stored at −20 °C before use.

Instrumentation and measurements

Generally, TEM images were recorded on a transmission electron microscope (HT-7700, Hitachi) at an acceleration voltage of 100 kV. 5 μL polymersome suspension (diluted 30 times with deionized water) was dropped onto a copper grid with carbon support films and dried in air. The hydrodynamic size distribution of the polymersomes was acquired on the particle size analyzer Zetasizer Nano ZS (Malvern Inc.). Absorbance spectra were measured using a UV–vis spectrometer (SPECORD 250 plus, Analytic Jena, AG, Germany). The response curves of ion-selective polymersomes to various cations were obtained in buffer at the indicated pH values with the gradual addition of the corresponding salt stock solutions. Fluorescence spectra were measured using a fluorescence spectrometer (Fluorolog-3, Horiba Jobin Yvon). Disposable poly(methyl methacrylate) cuvettes with a path length of 1 cm were used for absorbance and fluorescence measurements. Potentiometric signals were recorded on a precision electrochemistry interface (EMF-16, Lawson Laboratories Inc., USA).

Preparation of ion selective polymersomes

Typically, 1 mg of ABA, 0.05 mg of CH I (0.09 μmol), 0.24 mg of NaTFPB (0.27 μmol), and 0.28 mg Ca II (0.61 μmol) were dissolved in 800 μL EtOH to obtain a homogenous solution. The solution was pipetted and injected into 8 mL 20 mM pH 7.40 Tris-HCl buffer on a vortex at 1000 rpm. After removing EtOH by blowing compressed air on the surface, the clear Ca^{2+}-selective polymersome suspension was formed. To obtain the Na^+-selective polymersome suspension, an EtOH cocktail containing 2 mg of ABA, 0.05 mg of CH I (0.09 μmol), 0.24 mg of NaTFPB (0.27 μmol) and 0.65 mg Na X (0.65 μmol), and 20 mM pH 7.00 Tris-HCl buffer was used as the aqueous phase. Notice that 2 mg of ABA was used instead of 1 mg to fully incorporate the sensing components and avoid precipitation.

Preparation of the Ca^{2+}-selective electrode

1.5 mL THF solution of 2.2 mg Ca IV, 0.66 mg NaTFPB, 50 mg PVC, and 100 mg DD-NPE was poured into a glass ring with a 22 mm diameter on a glass slide. After evaporation of THF overnight at room temperature, the membrane was punched into disks of 8 mm diameter and conditioned in 1 mM $CaCl_2$ solution overnight. The conditioned membranes were mounted in commercial electrode bodies separately (Ostec, Sargans, Switzerland) with 1 mM $CaCl_2$ as the inner filling solution.

Purification of polymersome encapsulated hydrophilic dyes

The polymersomes encapsulating SRB were obtained by injecting the Ca^{2+}-selective polymersome cocktail into 1 mM SRB solution (in 20 mM pH 7.40 Tris-HCl buffer) on a vortex at 1000 rpm. After removing EtOH by blowing compressed air on the surface, a clear solution was obtained. To separate polymersomes containing entrapped SRB from free dyes, the solution was passed through the Sephadex G-25 column using 20 mM pH 7.40 Tris-HCl buffer as eluent.

Determination of total calcium level in serum

Ca^{2+}-selective polymersomes and Ca^{2+}-selective membrane electrodes (Ca^{2+} ISEs) were used to determine the total

calcium concentration in human serum, respectively. In the case of Ca^{2+}-selective polymersomes, the serum was first diluted 4 times with 20 mM pH 7.40 Tris-HCl buffer. Then, 1 μL of the diluted serum was injected into 1 mL polymersome suspension and the addition of known $CaCl_2$ (0, 0.5, 1, 1.5, 2, 2.5, and 3 μM) was followed stepwise. After each addition, the absorbance spectrum was recorded. Absorbance values at 670 nm were used in calculations. In the case of electrochemical measurements, potentiometric responses at different calcium concentrations were first recorded with a double-junction Ag/AgCl as the reference electrode (Metrohm AG, Switzerland) to establish the calibration curve. Afterward, 100 μL serum was added into 10 mL 10 mM pH 7.40 Tris-HCl buffer, and the potential values were recorded and used in calculations.

Results and discussion

As shown in Scheme 1, PMOXA–PDMS–PMOXA was used in this work for the self-assembly to form vesicles. The active sensing components (calcium ionophore II, chromoionophore I, and sodium tetrakis-[3,5-bis(trifluoromethyl)phenyl]-borate) were loaded into the lipophilic layer of polymersome membrane, resulting in Ca^{2+}-selective polymersomes. Na^{+}-selective polymersomes were prepared by simply replacing the types of ionophores (sodium ionophore X).

In previous works,[30,32–35] fabrication of relatively monodispersed ABA polymersomes often required sophisticated treatment such as extrusion after self-assembly. Here, we adopted a more convenient and rapid protocol to prepare the polymersomes based on the nanoprecipitation method. Uniform ABA vesicles were obtained by injecting the Ca^{2+}-selective cocktail into Tris-HCl buffer at pH 7.40. The vesicles were characterized with TEM and DLS. The TEM image (Fig. 1a) indicated the hollow structure of Ca^{2+}-selective polymersomes since higher contrast was observed on the peripheral. From the DLS results (Fig. 1b), the obtained vesicles exhibited a narrow particle size distribution with a polydispersity index (PDI) of 0.11 and an average hydrodynamic diameter of *ca.* 95 nm. The polymersomes exhibited excellent colloidal stability showing no flocculation over time even with high salt concentration.

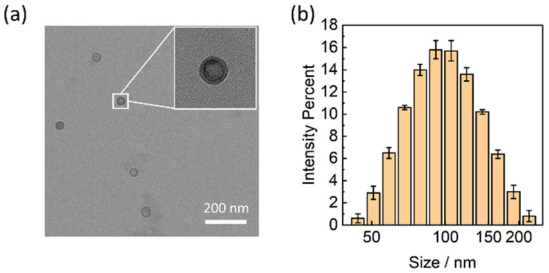

Fig. 1 A TEM image (a) and the hydrodynamic size distribution (b) of the Ca^{2+}-selective polymersomes.

Further confirmation of the vesicle formation was conducted by gel filtration chromatography on the Sephadex G-25 gel column. As shown in Fig. S1a,† the vesicles were eluted preferentially due to the size exclusion effect as expected and sufficiently separated from the free hydrophilic dye SRB. The different segments on the column were collected separately and the fluorescence emission spectra were evaluated. The fluorescence of the water-soluble SRB (575 nm, consistent with Fig. S1d†) and CH I (680 nm) were detected simultaneously in the purple solution (Fig. S1b†), indicating that the vesicles successfully encapsulated SRB in the hydrophilic cavity and CH I in the lipophilic layer. The polymersomes containing SRB exhibited an average hydrodynamic size of 105.1 nm (Fig. S1c†), which is comparable with that containing the calcium ionophores.

Fig. 2a shows the absorption spectra of the Ca^{2+}-selective polymersomes in the presence of different Ca^{2+} concentrations in Tris-HCl buffer solution (20 mM, pH 7.4). Initially, CH I was fully protonated without Ca^{2+} in the solution and the polymersomes appeared blue. With increasing calcium concentration, hydrogen ions on CH I were exchanged from the lipophilic layer into the aqueous phase, resulting in the deprotonation of CH I. Fig. 2b shows that the absorbance of the Ca^{2+}-selective polymersomes changed drastically in the range of 1 μM to 10 μM, and the limit of detection (LOD) was estimated to be 0.87 μM. The

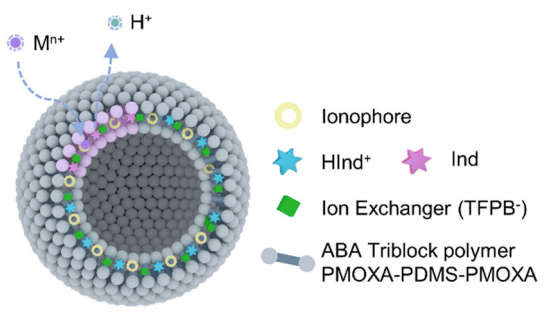

Scheme 1 Illustration of polymersome-based nano-ISOs. Polymersomes composed of the ABA triblock polymer PMOXA–PDMS–PMOXA were used to load the lipophilic ion sensing components in the membrane.

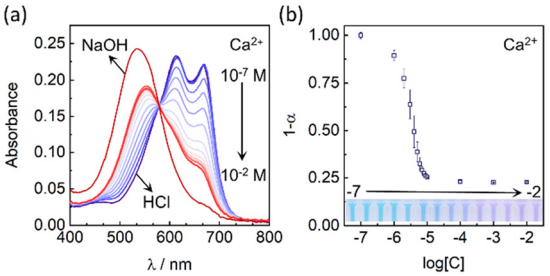

Fig. 2 (a) Absorbance spectra of the Ca^{2+}-selective polymersomes with various Ca^{2+} concentrations (Tris-HCl, 20 mM, pH 7.40). Acid and base indicate the spectra measured in the presence of HCl and NaOH, corresponding to the fully protonated and fully deprotonated states, respectively. (b) Calcium response corresponding to the experiments in (a) calculated based on the degree of protonation 1-α.

degree of protonation (1-α) decreased and stabilized around 0.23, indicating incomplete deprotonation of CH I. This could be explained by the protonation of CH I, regardless of ion-exchange, on the surface of polymersomes/nanospheres as previously investigated.[37,38]

The selectivity of the polymersome-based Ca^{2+} selective nano-ISOs was evaluated by measuring the optical response in the presence of various cations, respectively. The logarithmic selectivity coefficient $\log K_{i,j}$ was calculated from eqn (1) according to the literature,[39]

$$\log K_{i,j} = \log C_i - \log C_j \quad (1)$$

with i and j respectively representing the primary target ion and the interfering ion, and C_i and C_j respectively representing the concentration of the target ion and the interference ion at the response curve's midpoint (transition point). As shown in Fig. 3a, the polymersomes showed negligible response to the common interfering cations Na^+, K^+, Li^+, and Mg^{2+} up to 1 mM. Compared with the reported ion-selective nanospheres based on PVC, DOS, or lipids as the matrix material, the selectivity of the polymersome-based Ca^{2+} selective nano-ISOs was significantly improved, even for magnesium ions ($\log K_{Ca,Mg} = -4.17$, comparison of selectivity coefficients of other ions can be seen in Table S1†).

The Ca^{2+} response of the polymersomes was kinetically monitored at 670 nm (Fig. 3b), and the absorbance values were instantaneously stabilized after adding Ca^{2+}, indicating a rapid response. However, the optical response to Ca^{2+} appeared irreversible (Fig. S5†) upon the addition of the well-known chelators EGTA. This also means that the polymersomes are better suited as disposable analytical tools. The reason for the strange irreversibility could be linked to the unique vesicle structure and is still being investigated in the laboratory.

As a preliminary application, the Ca^{2+}-selective polymersomes were used to determine the total calcium concentration in human serum (see the Experimental section for details). Ca^{2+} selective ISEs (see preparation in the Experimental section) were used in external calibration mode as a control method. As shown in Fig. S2,† the total calcium concentration of the serum sample determined by

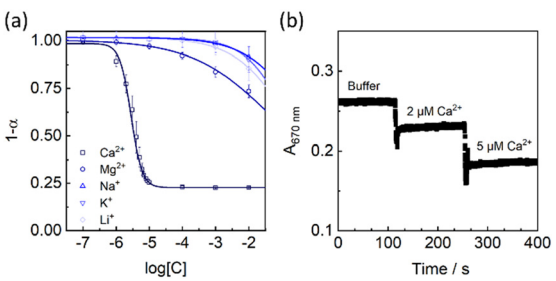

Fig. 3 (a) Selectivity patterns of the Ca^{2+}-selective polymersomes. (b) Kinetic response of the Ca^{2+}-selective polymersomes upon addition of different levels of Ca^{2+} as indicated.

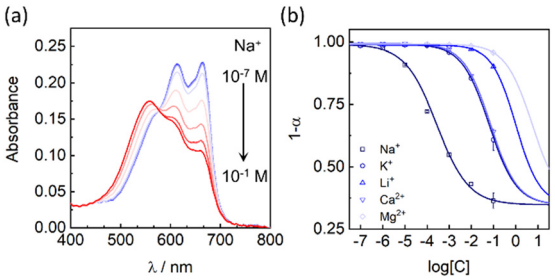

Fig. 4 (a) Absorbance spectra of the Na^+-selective polymersomes with various Na^+ concentrations in Tris-HCl buffer (20 mM, pH 7.00). (b) Selectivity patterns of the Na^+-selective polymersomes.

polymersomes was 2.24 mM, which was very close to that of the ISEs (2.19 mM). The total calcium concentration was also consistent with the normal range in healthy human serum (2.0 to 2.6 mM). Dilution was introduced in the measurements since the polymersomes were pre-dispersed in an aqueous solution, thus the results corresponded to the total calcium ion concentration instead of the ionized part. As described in previous studies, the hydrophilic layer formed by the self-assembly of PMOXA on the surface of vesicles endowed polymersomes a good anti-protein adsorption ability,[40] which further supported the *in vivo* bio-applications of the polymersome-based ISOs.

Finally, to confirm the generality of the ABA polymersomes as the matrix of ISOs, Na^+-selective polymersomes were also fabricated by replacing the calcium ionophore Ca II with the sodium ionophore Na X. As shown in Fig. 4, the polymersome-based Na^+-selective nano-ISOs exhibited a sigmoidal response to sodium ions from 1 μM to 0.1 M in Tris-HCl buffer of pH 7.0 with the LOD estimated to be 0.28 μM. Compared with previous research, the selectivity of the Na^+-selective polymersomes also was slightly improved ($\log K_{Na,K} = -2.4$ in this work). Selectivity coefficients of common interfering ions (K^+, Li^+, Ca^{2+}, and Mg^{2+}) were summarized in Table S2.† Compared with the Ca^{2+}-selective polymersomes, the Na^+ selective polymersomes exhibited a wider dynamic range, which could be explained by the different detection modes as previously described.[8] The Ca^{2+}-selective polymersomes contained the same ionophore which was used in previous ion-selective nanospheres in the exhaustive sensing mode, while the Na^+-selective polymersomes were operated in the equilibrium mode. This is the reason for the relative narrow dynamic range compared with the Na^+-selective polymersomes.

Conclusions

In summary, we introduced for the first time ABA polymersomes as the matrix to fabricate nano-ISOs without using additional plasticizers and surfactants. The uniform and clear polymersome solution was fabricated with the nanoprecipitation method. The polymersome-based nano-ISOs exhibited excellent sensitivity and selectivity as compared to several previous works. The results of Ca^{2+}-

selective polymersome determination of total calcium concentration in human serum proved its feasibility of testing practical samples. Ion-selective polymersomes for other ions could be realized by changing ionophores. As new topological nano-ISOs, much remains to be further explored, including understanding the role of the encapsulated aqueous phase. Besides, the vesicles could encapsulate both water-soluble dyes and lipophilic ion-sensing components, which may also be used for dual-functional chemical sensing purposes by simultaneously encapsulating appropriate hydrophilic small molecule probes and lipophilic sensing components.

Author contributions

X. Xie: conceptualization, writing – review & editing and funding acquisition. Y. Cui: investigation, methodology and validation – original draft. Y. Wang: investigation. J. Zhai: supervision, funding acquisition, writing – review & editing.

Conflicts of interest

There are no conflicts to declare.

Acknowledgements

This work was supported by the Department of Science and Technology of Guangdong Province (No. 2021A1515010330), the Shenzhen Science and Technology Program (No. 202110293000007), and the National Natural Science Foundation of China (No. 22274070).

Notes and references

1 E. Bakker, P. Buhlmann and E. Pretsch, *Chem. Rev.*, 1997, **97**, 3083–3132.
2 E. Zdrachek and E. Bakker, *Acc. Chem. Res.*, 2019, **52**, 1400–1408.
3 X. Xie, G. A. Crespo and E. Bakker, *Anal. Chem.*, 2013, **85**, 7434–7440.
4 X. Wang, M. Mahoney and M. E. Meyerhoff, *Anal. Chem.*, 2017, **89**, 12334–12341.
5 H. Shibata, Y. Hiruta and D. Citterio, *Analyst*, 2019, **144**, 1178–1186.
6 W. Di, X. Tan, I. A. C. Calderon, A. E. N. Reilly, M. Niedre and H. A. Clark, *Proc. Natl. Acad. Sci. U. S. A.*, 2020, **117**, 3509–3517.
7 X. Du and X. Xie, *Sens. Actuators, B*, 2021, **335**, 129368.
8 X. Xie and E. Bakker, *Anal. Bioanal. Chem.*, 2015, **407**, 3899–3910.
9 K. Klucinska, E. Stelmach, A. Kisiel, K. Maksymiuk and A. Michalska, *Anal. Chem.*, 2016, **88**, 5644–5648.
10 L. Deng, J. Zhai, X. Du and X. Xie, *ACS Sens.*, 2021, **6**, 1279–1285.
11 X. Du, M. Huang, R. Wang, J. Zhai and X. Xie, *Chem. Commun.*, 2019, **55**, 1774–1777.
12 X. Xie, J. Zhai, G. A. Crespo and E. Bakker, *Anal. Chem.*, 2014, **86**, 8770–8775.
13 X. Xie, I. Szilagyi, J. Zhai, L. Wang and E. Bakker, *ACS Sens.*, 2016, **1**, 516–520.
14 A. V. Kalinichev, A. Frosinyuk, M. A. Peshkova and K. N. Mikhelson, *Sens. Actuators, B*, 2017, **249**, 123–130.
15 M. M. Erenas, I. de Orbe-Paya and L. F. Capitan-Vallvey, *Anal. Chem.*, 2016, **88**, 5331–5337.
16 X. Du, J. Zhai, D. Zeng, F. Chen and X. Xie, *Sens. Actuators, B*, 2020, **319**, 128300.
17 X. Xie, G. Mistlberger and E. Bakker, *Anal. Chem.*, 2013, **85**, 9932–9938.
18 X. Xie, J. Zhai and E. Bakker, *J. Am. Chem. Soc.*, 2014, **136**, 16465–16468.
19 S. Apichai, L. Wang, K. Grudpan and E. Bakker, *Anal. Chim. Acta*, 2020, **1094**, 136–141.
20 J. M. Dubach, D. I. Harjes and H. A. Clark, *J. Am. Chem. Soc.*, 2007, **129**, 8418–8419.
21 X. Du, L. Yang, W. Hu, R. Wang, J. Zhai and X. Xie, *Anal. Chem.*, 2018, **90**, 5818–5824.
22 X. Du, R. Wang, J. Zhai, X. Li and X. Xie, *ACS Appl. Nano Mater.*, 2020, **3**, 782–788.
23 R. Wang, X. Du, Y. Wu, J. Zhai and X. Xie, *ACS Sens.*, 2018, **3**, 2408–2414.
24 M. J. Mitchell, M. M. Billingsley, R. M. Haley, M. E. Wechsler, N. A. Peppas and R. Langer, *Nat. Rev. Drug Discovery*, 2021, **20**, 101–124.
25 A. L. Dailey, M. D. Greer, T. Z. Sodia, M. P. Jewell, T. A. Kalin and K. J. Cash, *Biosensors*, 2020, **10**, 120.
26 E. Stelmach, E. Nazaruk, K. Maksymiuk and A. Michalska, *Anal. Chem.*, 2021, **93**, 13106–13111.
27 H. S. Rahman, H. H. Othman, N. I. Hammadi, S. K. Yeap, K. M. Amin, N. A. Samad and N. B. Alitheen, *Int. J. Nanomed.*, 2020, **15**, 2439–2483.
28 X. Zhang, P. Tanner, A. Graff, C. G. Palivan and W. Meier, *J. Polym. Sci., Part A: Polym. Chem.*, 2012, **50**, 2293–2318.
29 A. Moquin, J. Ji, K. Neibert, F. M. Winnik and D. Maysinger, *ACS Omega*, 2018, **3**, 13882–13893.
30 M. Kumar, M. Grzelakowski, J. Zilles, M. Clark and W. Meier, *Proc. Natl. Acad. Sci. U. S. A.*, 2007, **104**, 20719–20724.
31 F. Axthelm, O. Casse, W. H. Koppenol, T. Nauser, W. Meier and C. G. Palivan, *J. Phys. Chem. B*, 2008, **112**, 8211–8217.
32 M. Lomora, F. Itel, I. A. Dinu and C. G. Palivan, *Phys. Chem. Chem. Phys.*, 2015, **17**, 15538–15546.
33 O. Onaca, P. Sarkar, D. Roccatano, T. Friedrich, B. Hauer, M. Grzelakowski, A. Guven, M. Fioroni and U. Schwaneberg, *Angew. Chem., Int. Ed.*, 2008, **47**, 7029–7031.
34 D. Ho, S. Chang and C. D. Montemagno, *Nanomedicine*, 2006, **2**, 103–112.
35 M. Lomora, M. Garni, F. Itel, P. Tanner, M. Spulber and C. G. Palivan, *Biomaterials*, 2015, **53**, 406–414.
36 M. Lomora, I. A. Dinu, F. Itel, S. Rigo, M. Spulber and C. G. Palivan, *Macromol. Rapid Commun.*, 2015, **36**, 1929–1934.
37 X. Xie, J. Zhai, Z. Jarolimova and E. Bakker, *Anal. Chem.*, 2016, **88**, 3015–3018.
38 Q. Chen, J. Zhai, J. Li, Y. Wang and X. Xie, *Nano Res.*, 2022, **15**, 3471–3478.

39 G. Mistlberger, G. A. Crespo and E. Bakker, *Annu. Rev. Anal. Chem.*, 2014, **7**, 483–512.
40 A. Najer, A. B. Richards, H. Kim, C. Saunders, F. Fenaroli, C. Adrianus, J. Che, R. L. Tonkin, H. Hogset, S. Lorcher, M. Penna, S. G. Higgins, W. Meier, I. Yarovsky and M. M. Stevens, *Small*, 2022, **18**, 2201993.